2015-11-15

Improving the Electromechanical Performance of Dialectric Elastomers using Silicone Rubber and Dopamine Coated Barium Titanate.

Liang Jiang
Technological University Dublin

Tony Betts
Technological University Dublin, anthony.betts@tudublin.ie

David Kennedy
Technological University Dublin, david.kennedy@tudublin.ie

See next page for additional authors

Recommended Citation

Jiang, L. et al. (2015) Improving the Electromechanical Performance of Dialectric Elastomers using Silicone Rubber and Dopamine Coated Barium Titanate. *Materials and Design* Vol. 85, pp 733-742. DOI:10.1016/j.matdes.2015.07.075

Improving the Electromechanical Performance of Dielectric Elastomers using Silicone Rubber and Dopamine Coated Barium Titanate

Liang Jiang [a 1], Anthony Betts [b], David Kennedy [c], Stephen Jerrams [a]

[a] Centre for Elastomer Research, Focas Research Institute, Dublin Institute of Technology, Dublin 8, Ireland

[b] Applied Electrochemistry Group, Focas Research Institute, Dublin Institute of Technology, Dublin 8, Ireland

[c] Department of Mechanical Engineering, Dublin Institute of Technology, Dublin 1, Ireland

Abstract

In this work, a new soft dielectric elastomer (DE) was fabricated from dopamine coated barium titanate particles and silicone rubber (SR). The results show that the dopamine, in addition to coating the barium titanate ($BaTiO_3$, BT), the coated particles (DP-BT) were highly compatible with SR. In order to achieve a maximum voltage-induced deformation, the minimum secant moduli of DEs were obtained in experimentation at a stretch ratio of approximately 1.6 by applying equi-biaxial tensile strain using the bubble inflation method. Additionally, it was found that the addition of DP-BT into SR led to an increased dielectric constant and decreased dielectric loss tangent for the matrix by comparison with SR/BT composites. Furthermore, the electromechanical properties of the SR/DP-BT composites were greatly improved in terms of voltage-induced deformation (s_a), electromechanical energy density (e) and coupling efficiency (K^2). A maximum actuated area strain of approximately 78 %, which was 30 % larger than that of the SR/BT composites, was achieved for the sample having a DP-BT content of 20 wt%. This strain corresponded to a low dielectric strength of around 53 V/μm, the composite exhibited a maximum energy density of 0.07 MJ/m^3 and coupling efficiency of 0.68.

Keywords: Dielectric elastomers, Voltage-induced deformation, Equi-biaxial stretch, Energy density, Electromechanical coupling efficiency.

Introduction

DEs belong to a family of smart materials, having compliant electrodes sprayed on their surfaces, that can respond to electrical stimulus by changing their shapes [1]. The effective compressive stress (σ_v) is created by applying a high voltage between the top and bottom surfaces of the DE and complies with Eqn. (1).

$$\sigma_{\mathrm{V}} = \varepsilon'\varepsilon_0(\phi/z)^2 = \varepsilon'\varepsilon_0\varphi^2 \qquad (1)$$

where ε' is the relative permittivity or the dielectric constant of the DE material, ε_0 is the permittivity of the free space (8.85×10^{-12} F/m), φ is the electric field which equals the applied high voltage (Φ) divided by the thickness of the DE (z).

[1] Corresponding author, email: liang.jiang@mydit.ie

To date, both VHB acrylics [2, 3] and SR [4, 5] have been regarded as good candidates for DEs because they have provided the best characteristics when actuated. Hence, they have a large number of biomimicry applications such as refreshable braille devices [6], hand rehabilitation splints [7], microfluidic devices [8, 9] and wearable tactile interfaces [10, 11]. However, SR has begun to attract more interest as the DE matrix, because it does not have certain intrinsic limitations possessed by VHB acrylics such as low thermal stability, widely varying modulus with temperature change and high viscoelasticity [12, 13]. Furthermore, SR has superior biocompatibibility to most carbon based polymers [14]. It has been proven that voltage-actuated strain can be increased by increasing the dielectric constant of a composite while decreasing the elastic modulus (E) of the DE [15, 16]. The relation between dielectric constant and elastic modulus is described by Eqn. (2), when a constant elastic modulus exists for small strains (< 20%) and free boundaries are assumed [1, 17].

$$s_z = \varepsilon' \varepsilon_0 \varphi^2 / E \qquad (2)$$

Further, in order to investigate the relation between voltage and strain, numerous hyperelastic strain energy functions, such as the Neo-Hooken [18], Mooney-Rivlin [19], Ogden [20], Yeoh [21] and Gent [22, 23] models have been widely used to mathematically simulate DE behaviour. As the volume of a DE is assumed to be constant (Poisson's ratio $v \approx 0.5$) irrespective of whether a high voltage is applied or not, the area strain (s_a) has a simple relationship with the thickness strain as given by Eqn. (3).

$$s_a = 1/\left(1-|s_z|\right)-1 \qquad (3)$$

Therefore, high dielectric fillers with soft SR matrices offer the possibility of achieving large voltage-induced deformations. It has been reported that SR containing BT particles can produce a large area strain of around 30 % [24, 25] under a high voltage. Nevertheless, BT has a high dielectric loss tangent and poor compatibility with SR and these disadvantages prevent its further application in soft actuators. To negate this limitation, researchers focused on doping to modify BT [26, 27]. Dopamine, which can interact strongly with metal oxides by forming hydrogen bonds [4], was considered an effective chemical with which to modify the surface of BT particles [26, 28]. Moreover, both the aromatic group and the hydrogen bond are of high polorizability [29, 30] which is propitious to the enhancement of the dielectric constant.

The key to develop large strains in DE composites has been shown to be the application of pre-stretch [31-33]. Additionally, pre-stretch can reduce viscoelastic effects, thus improving mechanical efficiency and response time accompanied by a marginal decrease in the dielectric constant [34]. In elastomers, the mobility of molecular chains can be restricted by intermolecular interactions [35]. However, the intermolecular interactions can be reduced by stretching and this change is characterized by a reduction in elastic modulus. It was reported that a low elastic modulus is of benefit in allowing DE materials to achieve large voltage-induced deformations [36]. Though pre-stretch can also increase the dielectric strength [37], the strain-stiffening effect prevents large deformation in the electric field from occurring. On the basis of these considerations, it is potentially difficult to determine a pre-stretch for DEs to achieve large deformations. However, it is reasonable for a DE to obtain a larger deformation at a pre-stretch ratio which renders a minimum elastic modulus in the material in order to obtain the largest deformation when applying a constant electric field. In this study, the relation between elastic modulus and stretch was studied in equi-biaxial tensile tests using a bubble inflation system. Furthermore, dopamine coated BT was fabricated and the influence of introducing it to the

composite on the mechanical, dielectric and electromechanical properties of the DE was investigated.

Experimental

Materials

A commercial polymer, dimethylsiloxane (LSR4305 DEV, Bluestar Ltd., U.S.A), consisting of two parts (part A and part B) was used for fabricating the DE samples; NYOGEL 756G (Nye Lubricants, Inc., USA) was the conductive carbon grease used as the compliant electrode. Both BT and dopamine hydrochloride (melt point 248-250 °C) were purchased from Sigma-Aldrich Co. LLC. The average particle size of the BT was about 1 μm and the density was 6.08 g/ml at 25 °C.

Dopamine coated BT preparation

As shown in Fig. 1, 10 g of BT was dispersed in 50 ml of ethnol-water mixture having a mass ratio of 1:1 and stirred for 30 minutes in order to add an OH- functional group to the particle surfaces. The solution was then poured into 450 ml of deionized water and 1 g of dopamine hydrochloride was added. Thereafter, the suspension was stirred at 60 °C overnight before being subjected to ultrasonic shaking for 30 minutes. The dopamine coated BT was obtained by filtration, subsequently washed using deionized water and finally dried at 60 °C in a vacuum to avoid oxidization of the dopamine.

DE film preparation

Firstly, the two part of SR were mixed at a weight ratio of 1:1 and dissolved in heptane. Then, the BT or DP-BT particles, in the required weight percentage of 10 %, 20 % and 40 %, were added to the solution. In order to achieve uniform dispersion of the SR and fillers in heptane, the solution was subjected to ultrasonic shaking for 20 minutes. Finally, the mixture was poured into a watch glass, subjected to ultrasonic shaking for 30 minutes and heated for 3 hours at 80 °C in a water bath with an ultrasonic cleaner which performed the function of heating and shaking in an airing chamber. Fig. 1 shows that the dopamine coated BT had good compatibility with the SR matrix due to the hydrogen bond.

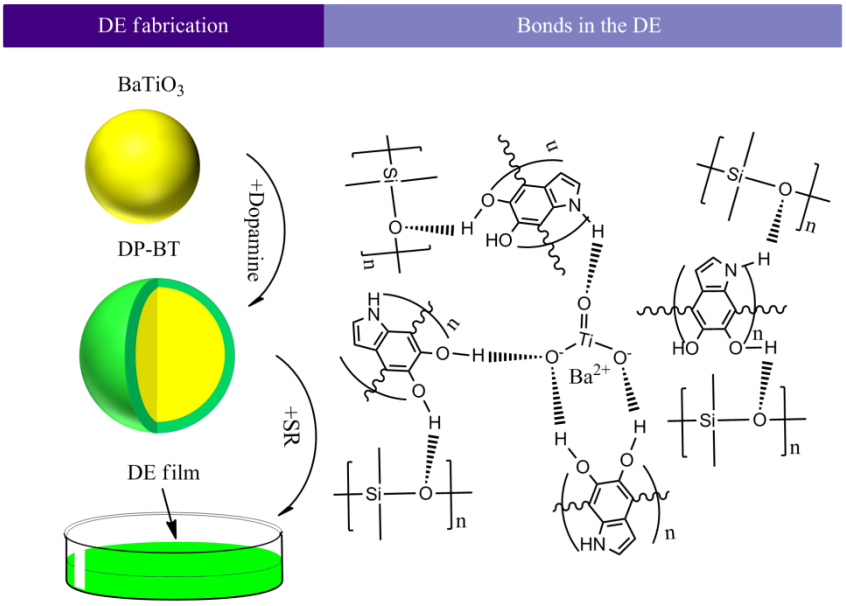

Fig. 1. Schematic of the fabrication of SR and dopamine coated BT composites.

This method can be readily incorperated into many widely used thin-film fabrication processes such as spin coating [38], doctor blade processes [39] and spray deposition [40]. Thin films with different thicknesses can be acquired by adjusting the amount of solvent.

Characterization

Fourier Transform Infrared Spectroscopy (FTIR) spectra of the BT and DP-BT micro-particles used in the experiment were recorded in the 650 - 4000 cm^{-1} range with a Perkin Elmer 400 Series Spectrometer.

The microstructures of all materials in this work were observed using a Scanning Electron Microscopy (SEM) (Zeiss Supra). Samples were coated with a fine layer of gold to make them conductive prior to observation. All images were taken with an accelerating voltage of 5 kV using a Secondary Electron (SE) detector.

The elemental analysis of these particle was carried out on an Energy Dispersive X-Ray Spectrometry (EDS) (Oxford Inca Xmax) which was coupled to the SEM.

Dielectric measurements of SR/BT and SR/DP-BT films were conducted on a Turnkey broadband dielectric spectrometer at 20 °C in the frequency range of 0.1 Hz to 10 MHz. The film of approximately 0.3 mm thickness was placed on a cell which was a disposable gold-plated flat electrode with a diameter of 20 mm and thickness of 2 mm.

The bubble inflation test system [41, 42] was designed for the equi-biaxial mechanical testing of elastomers by means of hydraulically inflating test samples using silicone oil. Disc samples of 50 mm nominal diameter were constrained in the bubble inflation system's inflation orifice. In the static tests, pressure was applied to the 2 mm thick samples causing them to inflate. The vision system, utilising two charge coupled device (CCD) cameras, recorded the movement of the centres of specific points at the pole on the surface of the samples during inflation. Stress values were simultaneously calculated from the applied pressure and bubble geometry, while strain values were calculated from the change in circumferential distance between the centres of

specific points on the bubble surface at the bubble pole, using three dimensional position coordinates obtained from the vision system output.

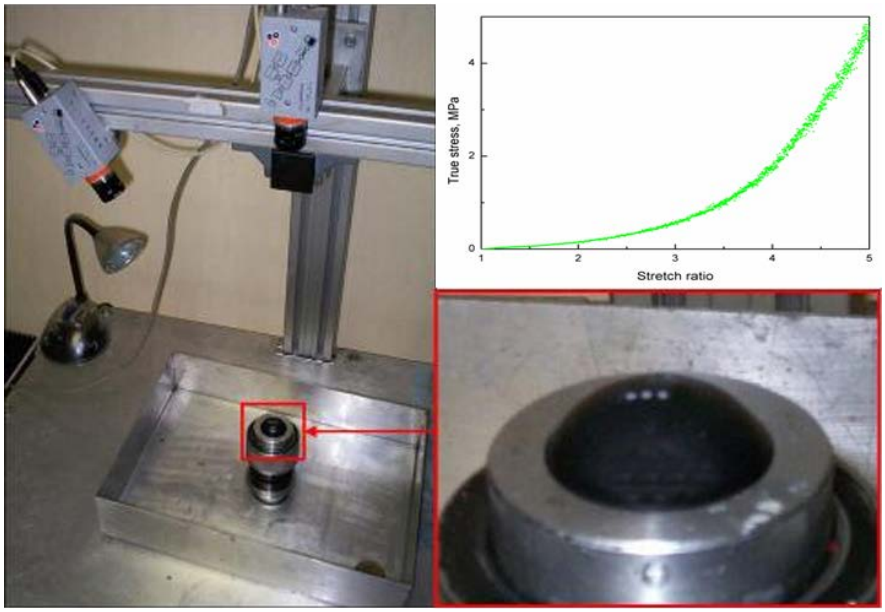

Fig. 2. A sample under test in the bubble inflation test system.

The voltage-induced deformations of all the composites were measured in the electromechanical test system, which consists of a camera, a biaxial clamp to apply pre-stretching and a high voltage power supply. Prior to use, these square samples were bonded in the clamping system and their sides were stretched in plane to a ratio λ_{pre}. The samples were then held at this pre-stretch in the clamps. The pre-stretched DE films were coated with the compliant electrode. Subsequently, DC voltages were applied with a ramped load increase of 0.5 kV per 10 seconds following a 10 seconds interval. A camera recorded area changes of the samples for each increment. Thereafter, the initial area (A_0) and the actuated area (A) were accurately measured using AutoCAD software. The area strain s_a was calculated from the following expression.

$$s_a = \left(A - A_0\right)/A_0 \qquad (4)$$

For the application of Eqn. (4) it is assumed that the two equal mutually perpendicular principal strains are orthogonal to the transverse (thickness) strain, Sz and are considered to be constant along their respective principal axes.

Results and Discussion

Microstructure and morphology of BT and DP-BT

The morphology of BT and DP-BT particles was studied using SEM. Figs. 3 (a) and (b) show the micrograph of BT and DP-BT respectively. It is evident that the BT particles have a uniform size of about 1 µm, while the shape of DP-BT particles was irregular and their surfaces rougher than that of the BT particles. This is mainly attributed to the growth of dopamine chains on the surface of BT particles.

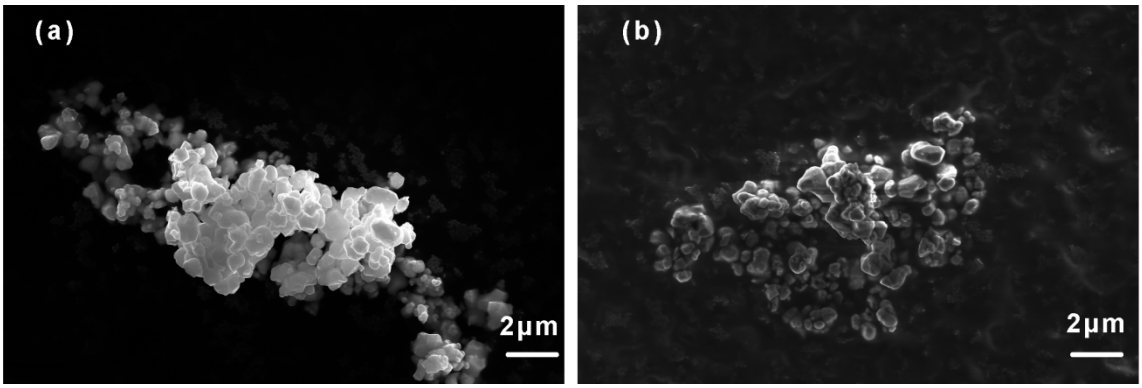

Fig. 3. SEM micrographs of particles used in the experiments: (a) BT; (b) DP-BT.

EDS analysis shows the presence of element Ba along with elements Ti and O indicating the fundamental constituents of BT. Carbon (C) was also detected in each of the particles, but there was a significant C background signal in BT due to the hydrocarbon (HC) contamination. This was possibly due to the chamber surfaces, vacuum pumps and sample surface migration and reaction with the electron beam to form a carbon rich environment [43]. However, the content of C in DP-BT (46 wt%) is more than that in BT (35 wt%) indicating the deposition of dopamine on BT particles. The content of element O changed only slightly after the deposition of dopamine with the O atomic mass fraction of dopamine nearly equal to that of BT.

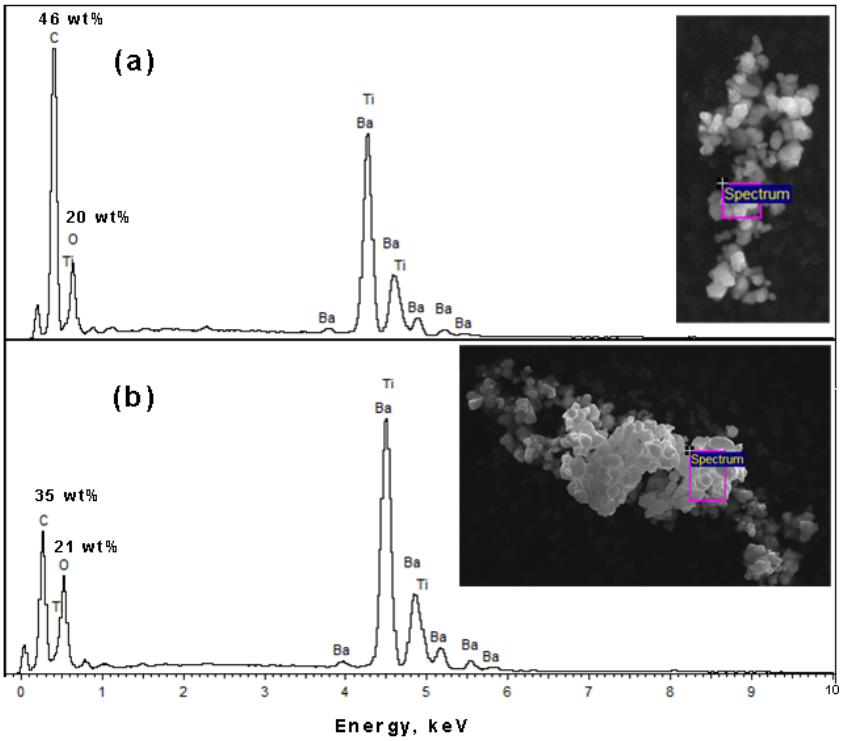

Fig. 4. EDS spectra of (a) DP-BT and (b) BT.

Fig. 5 shows the FT-IR transmittance spectra of BT and DP-BT. It can be observed that the transmittance intensity in the range from 650-4000 cm^{-1} was enhanced by coating BT with dopamine. Due to the deposition of dopamine on BT, the C-H bond appeared at 2916 cm^{-1}. The transmittance peaks located at 1607 cm^{-1} and 1286 cm^{-1} corresponded to aromatic amine N-H bending vibrations and C-N stretching vibrations respectively. In addition, the appearance of the peaks at 2568 cm^{-1} and 2168 cm^{-1} was interpreted as indicating the presence of the Ba-OH and Ti-OH [8] formatting which was probably due to the addition of ethanol during the fabrication of DP-BT.

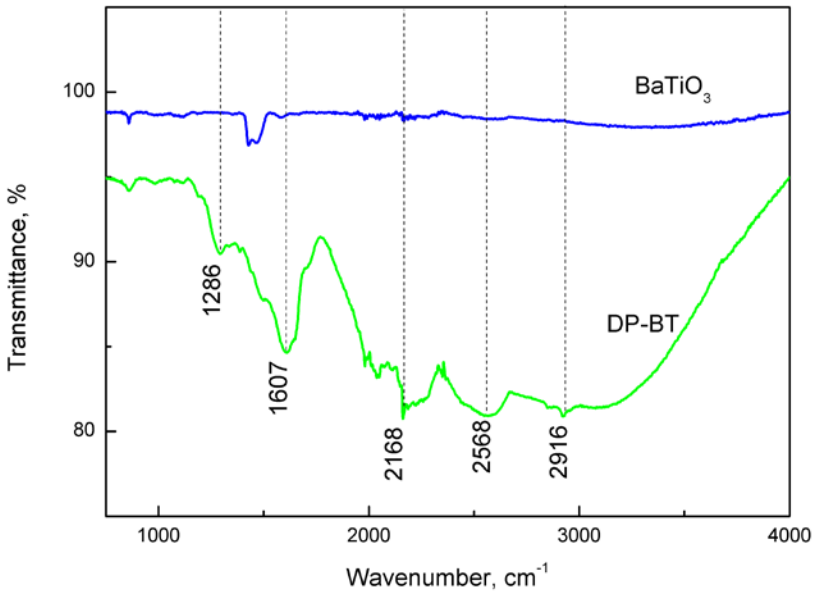

Fig. 5. FT-IR spectra of BT and DP-BT.

Microstructure of SR/BT and SR/DP-BT composites

Fig. 6 presents the microstructure of SR with BT and DP-BT composites respectively. As can be seen from the figure, some serious agglomeration of BT particles were exposed on the fractured surfaces of the compound. This can be attributed to the large difference in surface energy between the filler and matrix [28]. Conversely, very few agglomerates were found in the SR/DP-BT composites. With increasing DP-BT content, the packing of particles became denser which indicates an acceptable compatibility between DP-BT and the SR matrix. The SR/DP-BT composites exhibited good dispersibility even at the higher DP-BT content of 40 wt%. Moreover, the interface between DP-BT and SR was very indistinct indicating improved compatibility between the filler and the matrix due to the hydrogen bonds between dopamine and SR.

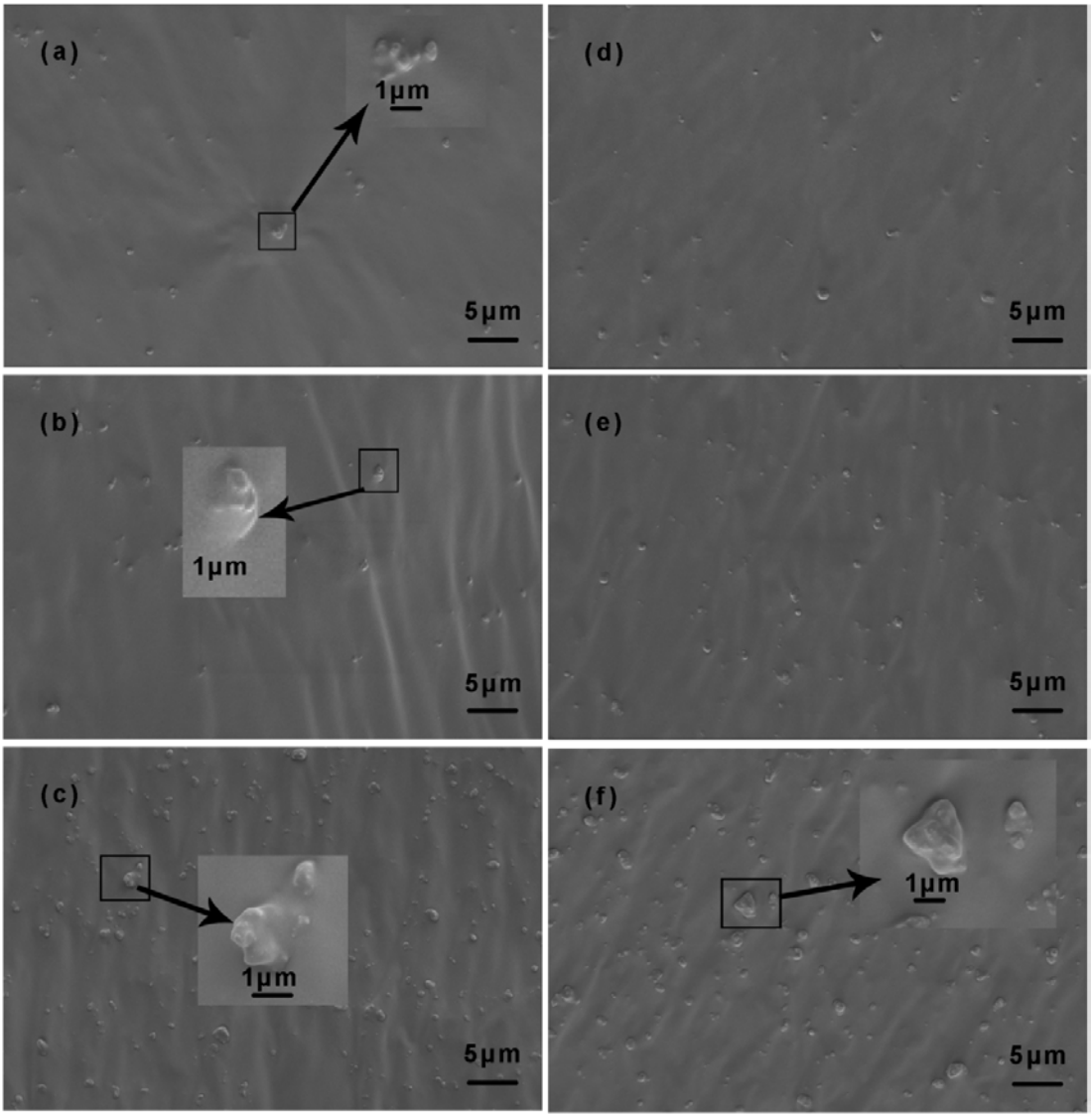

Fig. 6. SEM micrographs of SR based DE films with different content of BT and DP-BT, respectively: (a) 10 wt% BT; (b) 20 wt% BT; (c) 40 wt% BT; (d) 10 wt% DP-BT; (e) 20 wt% DP-BT; (f) 40 wt% DP-BT.

Mechanical properties of DE composites

The stress-stretch curves and secant modulus-stretch curves of SR composites with different BT and DP-BT contents are presented in Fig. 7. As shown in the figure, the true stresses of SR/DP-BT composites were in the approximate range of 3 MPa to 6 MPa for all films when subjected to an equi-biaxial stretch ratio of 5, while the stresses for the SR/BT composites were in the approximate range of 1.5 MPa to 8 MPa at the same stretch ratio and for the same particle contents. The true stress increased approximately linearly with the increases in stretch ratio for stretch areas from 1 to about 1.2 for both SR/BT and SR/DP-BT samples. The rate of increase in stress tended to be less for increases in stretch as the filler concentration increased indicating that stiffness generally and predictably reduced as filler loading increased. All samples used in this

test exhibited hyperelastic deformation. For the particle content range tested, it appeared that the 40 wt% of particle compounds were the weakest and the 10 wt% the strongest.

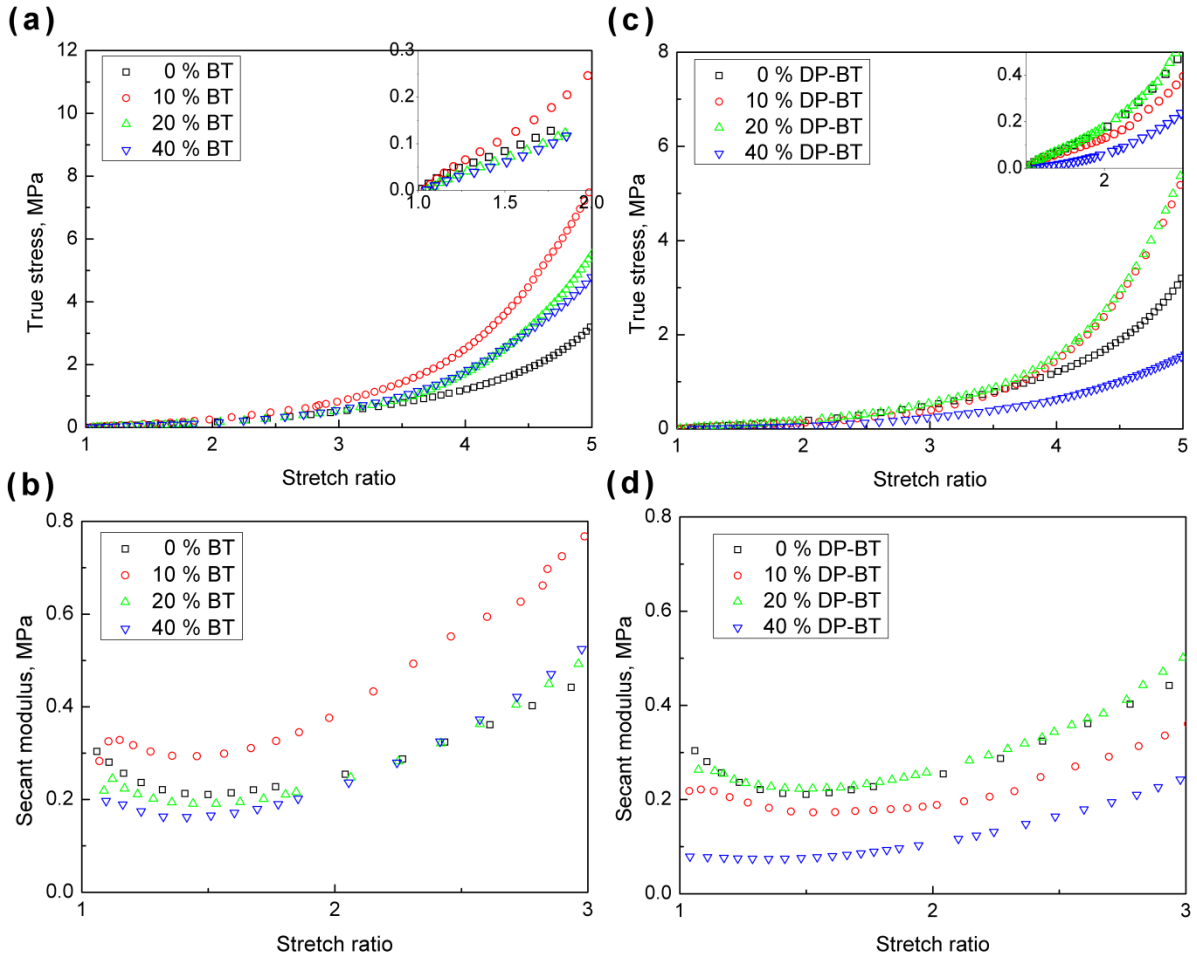

Fig. 7. Plots of true stress related to stretch for SR composites with various (a) BT content and (c) DP-BT contents; secant modulus of SRcomposites with varied filler content related to stretch ratio: (b) SR/BT composites and (d) SR/DP-BT composites.

The curves of secant modulus related to stretch ratio for SR/BT and SR/DP-BT composites are depicted in Figs. 7 (b) and (d) respecticely. The initial linear elastic portion of the stress-stretch curve is taken as the value of Young's modulus [44]. As stated, for all the DE composites, as observed in Figs. 7 (a) and (c), the linear stage occurred below a stretch ratio of 1.2 and it can be observed that the secant modulus approximately equals Young's modulus in this region. The stiffnesses of all the DE films used in the test was lower than that of the initial modulus of unfilled silicone (0.3 MPa). Furthermore, as shown in Figs. 7 (b) and (d), these secant modulus-stretch curves exhibit a material specific minimum in modulus indicating that their stiffness can be reduced by pre-stretching them to small ratios. This phenomenon is considered to be as a result of the influnce of intermolecular forces and chain entanglements between particles and matrices. It can be observed that the minimum elastic moduli were obtained at a stretch ratio of around 1.6 for both SR/BT and SR/DP-BT composites. This means that the application of an external force initially unravelled chain entanglement resulting in the elastic modulus firstly

falling at small stretch ratios. Thereafter, as the stretch ratio increased, intermolecular forces rose due to the hydrogen bonds between DP-BT and SR and the reorientation of molecular chains. In line with Eqn. (2), it is likely that a maxium voltage-induced area strain from pre-stretching can be obtained at a stretch ratio close to 1.6.

Dielectric constant and dielectric loss tangent of DE composites

Increasing the dielectric constant in a DE composite provides the opportunity to reduce the applied electric field in line with Eqn. (2). Fig. 8 shows the spectra of dielectric constant and dielectric loss tangent related to frequency for SR/BT composites and SR/DP-BT composites respectively. As can be observed from the Figs. 8 (a) and (c), unfilled SR possesses a dielectric constant of about 2.9 at 1 kHz and the dielectric constant ε' of both SR/BT composites and SR/DP-BT composites increased with the addition of filler content due to the strong presence of Maxwell-Wagner interfacial polarization [45, 46]. The composite of SR/DP-BT exhibits a maximum dielectric constant of approximately 7.9 at 1 kHz for a filler content of 40 wt%, which is larger than that of the SR composites with 40 wt% BT. All curves in the figure fluctuated slightly in the wide brand frequency range of 0.1 Hz to 1 MHz. The reason for this is probably because the particles bonded strongly with the matrices at low filler loadings and the molecular networks in the polymers restricted the mobility of molecurlar chains. Additionally, polymer chain entanglement was regarded as a factor in restricting the movement of polymer chains [25]. Furthermore, it seems likely that the amorphous SR was not influnced by dipole orientation at room temperature [47]. Thus, the dielectric constant was affected minimally by changes in frequecy. The dielectric loss tangent ($\tan\delta$) is often used to characterize the energy loss in dielectric materials. Figs. 8 (b) and (d) show the variation of loss tangent as a function of frequency for unfilled SR and the SR/BT and SR/DP-BT composites. All materials have a low loss tangent mainly due to the week polarizability of the silicone matrix [4].

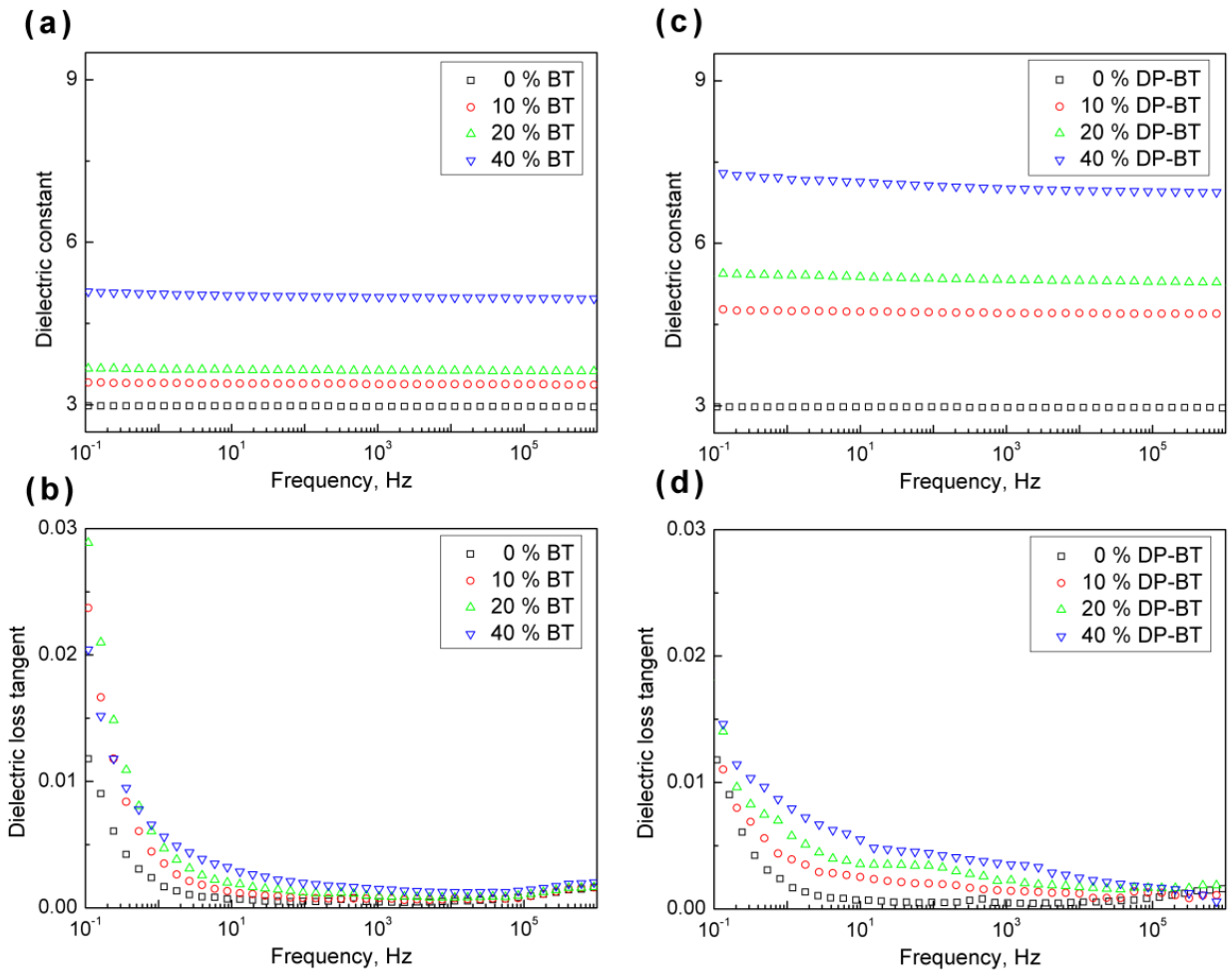

Fig. 8. Dielectric constant as a function of frequency for (a) SR/BT composites and (c) SR/DP-BT composites; dielectric loss tangent as a function of frequency for (b) SR/BT composites and (d) SR/DP-BT composites.

Figs. 9 (a) and (b) show the dielectric constant at 0.1 Hz and dielectric loss tangent at 0.1 Hz related to BT content and DP-BT content at room temperature. As can be observed from the figure, the dielectric constant of SR composites is increased with the enhancement of BT or DP-BT content. Also, the dielectric loss tangent decreased markedly for all samples up to a frequency of approximately 10 Hz. Unfilled silicone had the minimum loss tangent of about 0.012 at 0.1 Hz, while a maximum loss tangent of below 0.015 was achieved by the film with 40 wt% DP-BT. This is probably due to the presence of agglomerations and defects in the SR/DP-BT composites [25]. However, it can be seen that the dielectric loss tangent of SR composites was decreased by modifying BT.

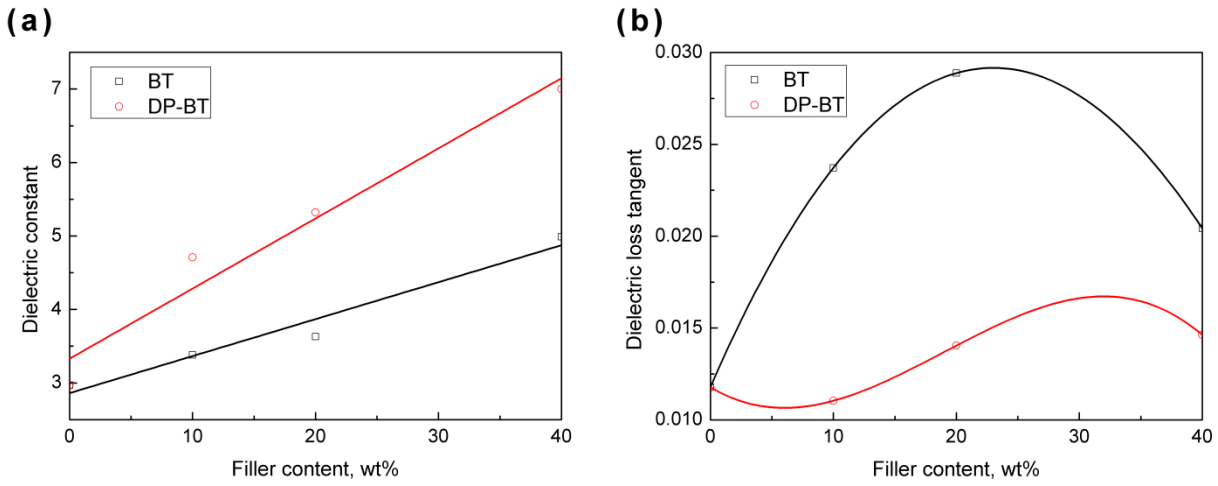

Fig. 9. Dielectric spectrum of BT and DP-BT versus filler content: (a) Dielectric constant; (b) dielectric loss tangent.

Voltage-induced strain of DE composites

The relation between actuated area strain and applied electric field for SR/BT composites and SR/DP-BT is shown in Fig. 10. Fig. 10 (a) depicts the working principle of DEs. Samples of silicone rubber doped with different filler loadings were bonded to equi-biaxial clamps to allow a pre-stretch ratio (λ_{pre}) of 1.6 in two mutually perpendicular planes to be applied prior to them being subjected to high voltages. From Figs. 10 (b) and (c), it can be observed that area strains for all samples subjected to high voltages (HV) increased greatly with increases in electric field strength. All the samples containing BT and DP-BT exhibited higher actuated area strains than the unfilled SR sample. The unfilled SR film achieved an area strain of 34 % with an applied electric field of 43 V/μm. For the SR/DP-BT composites, the sample with 20 wt% DP-BT exhibited the maximum deformation of about 78 % for the application of an electric field of around 53 V/μm. Though silicone rubber with 20 wt% BT achieved a relatively small area strain of around 57 % under an electric field of 46 V/μm, this was the maximum value reached by any of the SR/BT composite samples. It also can be seen that the voltage-induced strains of the SR composites with fillers were larger than those of the unfilled SR samples for the same electric field strength due to the effect of the increased dielectric constant of the SR composites. Moreover, the incorporation of BT and DP-BT enhanced the breakdown strength of DE composites. This is in accordance with previous research into other polymer-based composites [48, 49].

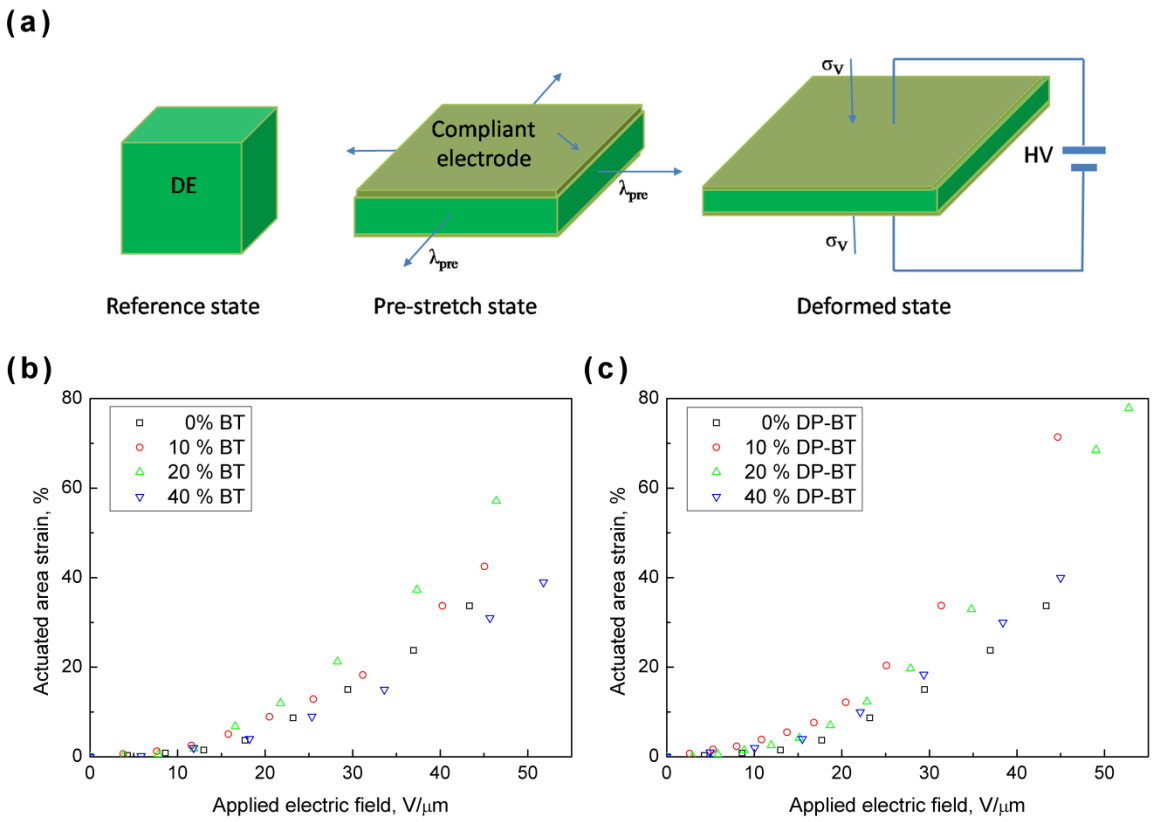

Fig. 10. (a) The working principle of DEs; the actuated area strain of (b) SR/BT composites and (c) SR/DP-BT composites related to the applied electric field.

For all samples, area strain increased as the voltage applied to the surfaces of the DE samples increased. The electromechanical sensitivity (β), which is the ratio of dielectric constant to elastic modulus, was regarded as a significant value in the determination of the voltage induced deformations [28]. As can be seen from Fig. 11, the sensitivity increased with increasing BT and DP-BT content in all the SR composites. However, the sticky film applied to the SR with 40 wt% DP-BT had the maximum sensitivity but didn't result in the largest voltage-induced area strain. This was probably due to electrode instability and the sample having inherent material defects [28] such as the agglomerations referred to Fig. 6. Voids may also have been present in the samples.

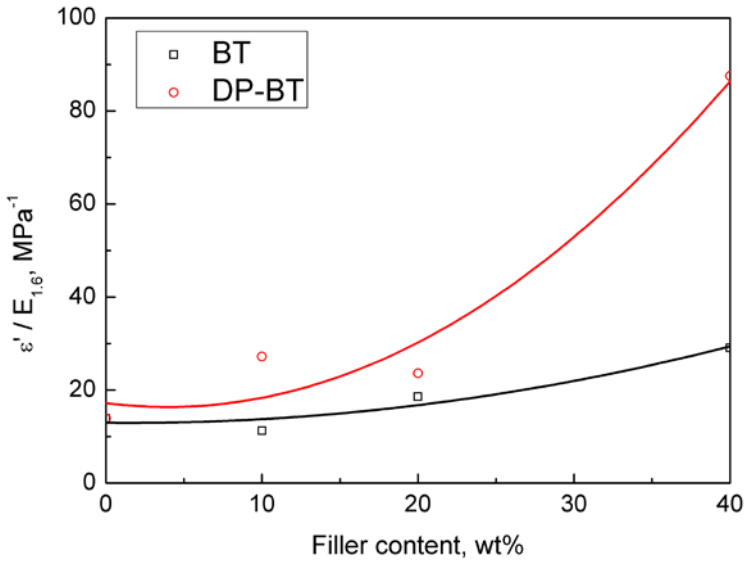

Fig. 11. The ratio of dielectric constant to secant modulus at λ_{pre} = 1.6 related to the BT and DP-BT mass ratios of SR composites.

In a DE, electromechanical energy density (e) is the amount of work generated in one actuation cycle per unit volume of actuator. The electromechanical coupling efficiency (K^2) is the electrical energy converted into mechanical energy per cycle, so is a measure of the electrical energy that needs to be supplied to provide a level of mechanical energy (or physical actuation). Each parameter is of key importance for characterizing the energy efficiency produced by a DE. 'e' and 'K^2'are obtained from Eqns. (4) and (5) [14] respectively.

$$e = -\sigma_V \ln\left(1-|s_z|\right) \quad (4)$$

$$K^2 = 2|s_z| - s_z^2 \quad (5)$$

The dependence of electromechanical energy density and coupling efficiency on filler content is shown in Fig. 12. The DE with added BT exhibited a largest energy density of 0.04 MJ/m^3 at a filler loading of 40 wt% and a maximum electromechanical coupling efficiency of 0.59 at a filler loading of 20 wt%. However, a SR composite with 20 wt% DP-BT obtained a maximum energy density of 0.07 MJ/m^3 and had a maximum electromechanical coupling efficiency of 68 %.

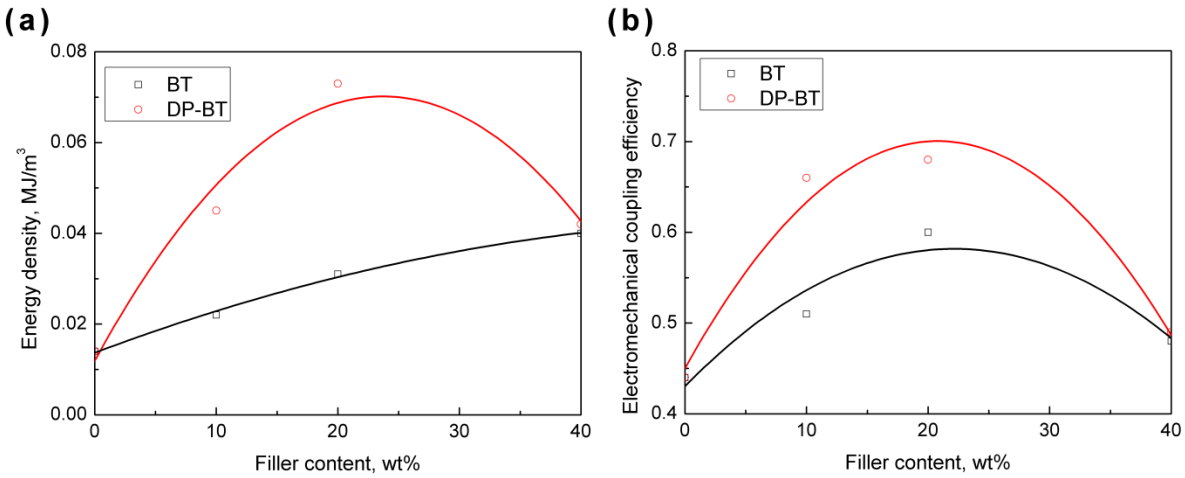

Fig. 12. The dependence of (a) electromechanical energy density and (b) electromechanical coupling efficiency on BT and DP-BT content

Conclusions

The modified BT using dopamine exhibits high compatibility with the SR matrix due to the presence of hydrogen bonds. Also, the elastic moduli for all composites used in this work were very small allowing them to achieve high area strains when high electric fields were applied. Prior to the application of the electric fields, the key pre-stretch ratio of 1.6 was determined by means of equi-biaxial mechanical testing. By comparison with conventional uniaxial testing, the method described here is more accurate in defining the optimum mechanical properties for loading DE specimens. Furthermore, the dielectric constant of the SR based composites was increased by filling the SR samples with dopamine coated BT, while the dielectric loss tangent was decreased. Finally, the SR composites with 20 wt% DP-BT displayed the highest electromechanical performance in terms of a maximum voltage-induced area strain of 78 % together with an electromechanical energy density of 0.07 MJ/m^3 and coupling efficiency of 0.68.

Acknowledgements

The authors gratefully acknowledges the support provided by the DIT Fiosraigh Dean of Graduate Students Award.

References

[1] R. Pelrine, R. Kornbluh, Q. Pei, J. Joseph, High-Speed Electrically Actuated Elastomers with Strain Greater Than 100%, Science, 287 (2000) 836-839.
[2] R. Pelrine, R. Kornbluh, J. Joseph, R. Heydt, Q. Pei, S. Chiba, High-field deformation of elastomeric dielectrics for actuators, Materials Science and Engineering: C, 11 (2000) 89-100.
[3] S. Michel, X.Q. Zhang, M. Wissler, C. Löwe, G. Kovacs, A comparison between silicone and acrylic elastomers as dielectric materials in electroactive polymer actuators, Polymer International, 59 (2010) 391-399.

[4] M.-F. Lin, V.K. Thakur, E.J. Tan, P.S. Lee, Surface functionalization of BaTiO3 nanoparticles and improved electrical properties of BaTiO3/polyvinylidene fluoride composite, RSC Advances, 1 (2011) 576-578.
[5] T. Vu-Cong, C. Jean-Mistral, A. Sylvestre, Impact of the nature of the compliant electrodes on the dielectric constant of acrylic and silicone electroactive polymers, Smart Materials and Structures, 21 (2012) 105036.
[6] K. Ren, S. Liu, M. Lin, Y. Wang, Q.M. Zhang, A compact electroactive polymer actuator suitable for refreshable Braille display, Sensors and Actuators A: Physical, 143 (2008) 335-342.
[7] G. Mondin, M. Haft, F.M. Wisser, A. Leifert, N. Mohamed-Noriega, S. Dörfler, S. Hampel, J. Grothe, S. Kaskel, Investigations of mussel-inspired polydopamine deposition on WC and Al_2O_3 particles: The influence of particle size and material, Materials Chemistry and Physics, 148 (2014) 624-630.
[8] M. Bhuiyan, M. Alam, M. Momin, M. Uddin, M. Islam, Synthesis and characterization of barium titanate ($BaTiO_3$) nanoparticle, International Journal of Material and Mechanical Engineering, 1 (2012) 21.
[9] M. Giousouf, G. Kovacs, Dielectric elastomer actuators used for pneumatic valve technology, Smart Materials and Structures, 22 (2013) 6.
[10] H.R. Choi, D. Kim, N.H. Chuc, N.H.L. Vuong, J. Koo, J.D. Nam, Y. Lee, Development of integrated tactile display devices, Proc. SPIE. 7287, Electroactive Polymer Actuators and Devices (EAPAD) 2009, 72871C (2009).
[11] K. Ig Mo, J. Kwangmok, K. Ja-Choon, J.D. Nam, L. Young Kwan, C. Hyouk-Ryeol, Development of Soft-Actuator-Based Wearable Tactile Display, Robotics, IEEE Transactions on, 24 (2008) 549-558.
[12] J.J. Sheng, H.L. Chen, L. Liu, J.S. Zhang, Y.Q. Wang, S.H. Jia, Dynamic electromechanical performance of viscoelastic dielectric elastomers, Journal of Applied Physics, 114 (2013) 8.
[13] S. Rosset, B.M. O'Brien, T. Gisby, D. Xu, H.R. Shea, I.A. Anderson, Self-sensing dielectric elastomer actuators in closed-loop operation, Smart Materials and Structures, 22 (2013) 104018.
[14] R. Shankar, T.K. Ghosh, R.J. Spontak, Dielectric elastomers as next-generation polymeric actuators, Soft Matter, 3 (2007) 1116-1129.
[15] D. Yang, M. Tian, H. Kang, Y. Dong, H. Liu, Y. Yu, L. Zhang, New polyester dielectric elastomer with large actuated strain at low electric field, Materials Letters, 76 (2012) 229-232.
[16] M. Tian, Y. Yao, S. Liu, D. Yang, T. Nishi, L. Zhang, N. Ning, Separated-structured all-organic dielectric elastomer with large actuation strain under ultralow-voltage and high mechanical strength, Journal of Material Chemistry A, (2014).
[17] D. Yang, M. Tian, Y.C. Dong, H.L. Kang, D.L. Gong, L.Q. Zhang, A high-performance dielectric elastomer consisting of bio-based polyester elastomer and titanium dioxide powder, Journal of Applied Physics, 114 (2013) 9.
[18] L. Zhang, Q. Wang, X. Zhao, Mechanical constraints enhance electrical energy densities of soft dielectrics, Applied Physics Letters, 99 (2011), 171906.
[19] Y. Liu, L. Liu, K. Yu, S. Sun, J. Leng, An investigation on electromechanical stability of dielectric elastomers undergoing large deformation, Smart Materials Structures, 18 (2009) 095040.
[20] Y. Liu, L. Liu, Z. Zhang, J. Leng, Dielectric elastomer film actuators: characterization, experiment and analysis, Smart Materials and Structures, 18 (2009) 095024.
[21] A. Schmidt, P. Rothemund, E. Mazza, Multiaxial deformation and failure of acrylic elastomer membranes, Sensors and Actuators A: Physical, 174 (2012) 133-138.

[22] B. Li, L. Liu, Z. Suo, Extension limit, polarization saturation, and snap-through instability of dielectric elastomers, International Journal of Smart and Nano Materials, 2 (2011) 59-67.
[23] C. Keplinger, T. Li, R. Baumgartner, Z. Suo, S. Bauer, Harnessing snap-through instability in soft dielectrics to achieve giant voltage-triggered deformation, Soft Matter, 8 (2012) 285-288.
[24] Z. Zhang, L. Liu, J. Fan, K. Yu, Y. Liu, L. Shi, J. Leng, New silicone dielectric elastomers with a high dielectric constant, Proc. SPIE, Modeling, Signal Processing and control for Smart Structures 2008, (2008) 692610.
[25] M. Takala, Electrical insulation materials towards nanodielectrics, Tampere University of Technology. Publication; 928, (2010).
[26] B.C. Luo, X.H. Wang, Y.P. Wang, L.T. Li, Fabrication, characterization, properties and theoretical analysis of ceramic/PVDF composite flexible films with high dielectric constant and low dielectric loss, Journal of Material Chemistry A, 2 (2014) 510-519.
[27] P. Kim, S.C. Jones, P.J. Hotchkiss, J.N. Haddock, B. Kippelen, S.R. Marder, J.W. Perry, Phosphonic Acid-Modified Barium Titanate Polymer Nanocomposites with High Permittivity and Dielectric Strength, Advanced Materials, 19 (2007) 1001-1005.
[28] D. Yang, M. Tian, D. Li, W. Wang, F. Ge, L. Zhang, Enhanced dielectric properties and actuated strain of elastomer composites with dopamine-induced surface functionalization, Journal of Material Chemistry A, 1 (2013) 12276-12284.
[29] P. Ren, C. Wu, J.W. Ponder, Polarizable atomic multipole-based molecular mechanics for organic molecules, Journal of chemical theory and computation, 7 (2011) 3143-3161.
[30] R. Janoschek, E.G. Weidemann, H. Pfeiffer, G. Zundel, Extremely high polarizability of hydrogen bonds, Journal of the American Chemical Society, 94 (1972) 2387-2396.
[31] J. Qiang, H. Chen, B. Li, Experimental study on the dielectric properties of polyacrylate dielectric elastomer, Smart Materials and Structures, 21 (2012) 025006.
[32] S.J.A. Koh, T. Li, J. Zhou, X. Zhao, W. Hong, J. Zhu, Z. Suo, Mechanisms of large actuation strain in dielectric elastomers, Journal of Polymer Science Part B: Polymer Physics, 49 (2011) 504-515.
[33] H. Tianhu, M. Guanghong, C. Cheng, The effect of prestretch on the performance of a dielectric elastomer membrane, Remote Sensing, Environment and Transportation Engineering (RSETE), 2011 International Conference on, (2011) 6463-6467.
[34] P. Brochu, Q. Pei, Advances in Dielectric Elastomers for Actuators and Artificial Muscles, Macromolecular Rapid Communications, 31 (2010) 10-36.
[35] K. Makuuchi, S. Cheng, Radiation processing of polymer materials and its industrial applications, John Wiley & Sons2012.
[36] X. Zhao, Q. Wang, Harnessing large deformation and instabilities of soft dielectrics: Theory, experiment, and application, Applied Physics Reviews, 1 (2014) -.
[37] Z. Suo, Theory of dielectric elastomers, Acta Mech. Solida Sin., 23 (2010) 549-578.
[38] P. Lotz, M. Matysek, H.F. Schlaak, Fabrication and Application of Miniaturized Dielectric Elastomer Stack Actuators, Mechatronics, IEEE/ASME Transactions on, 16 (2011) 58-66.
[39] A.I. Kontos, A.G. Kontos, D.S. Tsoukleris, M.-C. Bernard, N. Spyrellis, P. Falaras, Nanostructured TiO2 films for DSSCS prepared by combining doctor-blade and sol–gel techniques, Journal of Materials Processing Technology, 196 (2008) 243-248.
[40] O.A. Araromi, A.T. Conn, C.S. Ling, J.M. Rossiter, R. Vaidyanathan, S.C. Burgess, Spray deposited multilayered dielectric elastomer actuators, Sensors and Actuators A: Physical, 167 (2011) 459-467.

[41] R.F. Landel, L.E. Nielsen, Mechanical Properties of Polymers and Composites, Second Edition, Taylor & Francis1993.
[42] S. Jerrams, N. Murphy, J. Hanley, The significance of equi-biaxial bubble inflation in determining elastomeric fatigue properties, Published in the book Elastomers edited by Anna Boczkowska (ISBN 979-953-307-1019-5), InTech, (2012).
[43] P. Rolland, V. Carlino, R. Vane, Improved Carbon Analysis with Evactron Plasma Cleaning, Microscopy and Microanalysis, 10 (2004) 964-965.
[44] A.J. Kulkarni, M. Zhou, F.J. Ke, Orientation and size dependence of the elastic properties of zinc oxide nanobelts, Nanotechnology, 16 (2005) 2749.
[45] C. Putson, D. Jaaoh, N. Muensit, Interface Polarization Effect on Dielectric and Electrical Properties of Polyurethane (PU)/Polyaniline (PANI) Polymer Composites, Advanced Materials Research, 770 (2013), 275-278.
[46] G. Gallone, F. Carpi, D. De Rossi, G. Levita, A. Marchetti, Dielectric constant enhancement in a silicone elastomer filled with lead magnesium niobate–lead titanate, Materials Science and Engineering: C, 27 (2007) 110-116.
[47] M. Sharma, G. Madras, S. Bose, Process induced electroactive [small beta]-polymorph in PVDF: effect on dielectric and ferroelectric properties, Physical Chemistry Chemical Physics, 16 (2014) 14792-14799.
[48] Y. Song, Y. Shen, H. Liu, Y. Lin, M. Li, C.W. Nan, Improving the dielectric constants and breakdown strength of polymer composites: effects of the shape of the BaTiO3 nanoinclusions, surface modification and polymer matrix, Journal of Materials Chemistry, 22 (2012) 16491-16498.
[49] S. Bose, P. Mahanwar, Effect of particle size of filler on properties of nylon-6, Journal of Minerals & Materials Characterization & Engineering, 3 (2004) 23-31.